Eur. Phys. J. B **9**, 299–307 (1999)

THE EUROPEAN PHYSICAL JOURNAL B

EDP Sciences

Unbounded fluctuations in transport through an integrable cavity

P. Pichaureau[1] and R.A. Jalabert[1,2,a]

[1] Institut de Physique et Chimie des Matériaux de Strasbourg, 23 rue du Loess, 67037 Strasbourg Cedex, France
[2] Université Louis Pasteur, 3-5 rue de l'Université, 67084 Strasbourg Cedex, France

Received 17 July 1998 and Received in final form 23 November 1998

Abstract. We derive a semiclassical scheme for the conductance through a rectangular cavity. The transmission amplitudes are expressed as a sum over families of trajectories rather than a sum over isolated trajectories. The contributing families are obtained from the evaluation of a finite number of continued fractions. We find that, contrary to the chaotic case, the conductance fluctuations increase with the incoming energy and the correlation function exhibits a singularity at the origin.

PACS. 73.23.Ad Ballistic transport – 03.65.Sq Semiclassical theories and applications

1 Introduction

The density of states of small quantum systems is known to be sensitive to the underlying classical mechanics. The chaotic or integrable character of the classical dynamics translates into the statistical properties of the spectra [1]. The spectral correlations of classically chaotic systems are described according to random matrix theory [2] and the fluctuations with respect to the mean density of states are less pronounced than for integrable systems. The connection between classical and quantum properties is particularly clear within the semiclassical approximation: the density of states of classically chaotic systems is expressed in the Gutzwiller trace formula [3] as a sum over [isolated] periodic orbits, while integrable systems are described by the Berry-Tabor formula [4], where the the density of states is given as a sum over families of trajectories (or invariant tori).

What is the corresponding situation in open systems? Transport properties instead of spectral ones are usually considered. The transmission amplitudes and probabilities are given as semiclassical expansions over trajectories that traverse the scattering region [5,6], providing a link between classical and quantum properties. Such an approach is firmly established in the case of isolated trajectories, as typically found for chaotic dynamics, but only recently the subtleties associated with an integrable geometry have started to be addressed [7–11]. As in the Berry-Tabor formula for the density of states, the existence of families of trajectories degenerate in action modifies the structure of the semiclassical expansion. Integrable cavities fed by leads present the additional problem that conserved quantities in the scattering region are not necessarily conserved in the leads. The semiclassical description of transport through integrable cavities is a necessary step towards understanding the influence of the underlying classical mechanics in open systems. This is the goal of this work, where we present a semiclassical evaluation of the transmission amplitude through a rectangular cavity and apply it to the study of the conductance fluctuations.

The interest in open systems stems from their parallel with closed systems and also from the physically measurable realizations that have been developed in the last few years. High mobility-semiconductor microstructures at low temperatures give access to the ballistic regime, where transport is dominated by the geometrical scattering of electrons off the walls of the lithographically defined cavities [12–14]. On the other hand, microwave cavities provide an easily tunable system to study the propagation of electromagnetic waves in a defect-free region [15].

Quantum interference in ballistic cavities gives rise to conductance fluctuations under a small perturbation of the system (magnetic field, Fermi energy of the incoming electrons, shape of the cavity, etc.) [12,16,17]. For chaotic cavities, the characteristic correlation lengths of the fluctuations are well-described by the existing semiclassical theories [6,18], while the universal character of the variance has been addressed within a Dyson hypothesis for the scattering matrix [19,20]. Random matrix theories are obviously not appropriate to treat integrable systems, forcing us to rely on semiclassical expansions and numerical calculations. The early experiments on ballistic cavities [12] yielded a more structured spectrum of conductance fluctuations for the integrable case than for the chaotic one. This tendency was reproduced by numerical calculations [7] showing that in rectangular cavities the higher harmonics of the conductance spectrum are more pronounced than in the chaotic case. Also, the variance of the conductance appeared as increasing with the mode number. The lack of transport theories for integrable

[a] e-mail: jalabert@grannus.u-strasbg.fr

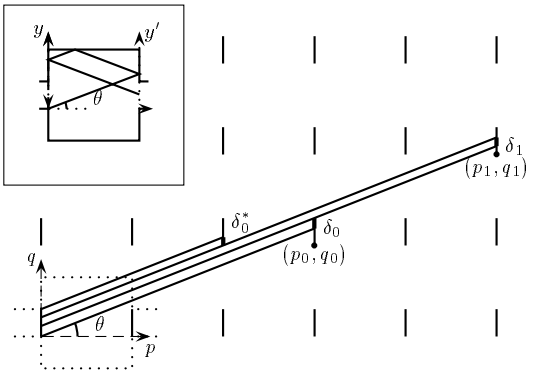

Fig. 1. Unfolded space for the dynamics in a square cavity (inset). The trajectory entering at the lowest point ($y = 0$) of the left lead with an angle θ is shown in the original and extended space. It belongs to the family that leaves the cavity through the exiting lead (p_0, q_0) and has a weight δ_0. For the particular chosen θ there are two families contributing to the transmission amplitude (0 and 1) and one family contributing to the reflection amplitude (0^*).

systems (which do not enjoy the universality properties of chaotic cavities) and the difficulties with their fabrication are probably responsible for the fact that subsequent efforts on conductance fluctuations were mainly centered on the chaotic case [21].

Weak-localization, the decrease of the average conductance due to constructive interference of time-reversed backscattering trajectories, is another quantum interference effect which has recently been studied in ballistic cavities. The underlying classical mechanics was proposed [22] to translate into a different shape of the magnetoconductance peaks: a Lorentzian line-shape for chaotic cavities and a triangular form for the integrable case. Chaotic cavities indeed exhibited the Lorentzian line-shape while rectangular and circular geometries showed triangular or Lorentzian peaks depending on the experiment [16,17,23–25]. The importance of the leads has been demonstrated [26] and the disagreements between different experiments are not settled yet. This illustrates the difficulties in dealing with integrable cavities and the importance of developing appropriate theoretical descriptions.

In this work we consider a square cavity (of length side 1) with hard walls and connected to leads on opposite sides of the square by openings of size W (see inset Fig. 1). (For our purposes square cavities are no less general than rectangular ones since we can always scale one of the sides.) We develop in Section 2 a semiclassical expansion of the transmission amplitude between two modes in terms of families of trajectories degenerate in action. The determination of these families (Sect. 3) results in a diophantic problem and the evaluation of a finite number of continued fractions. This constitutes a very efficient numerical method that is to be compared with the numerical quantum approaches based on discretization of real space or truncation of Hilbert space. The classical conductance (Sect. 4) and the unbounded fluctuations (Sect. 5), increasing with the incoming energy, are obtained from the numerical implementation of the continued fraction approach. The correlation function of the conductance, when properly normalized, is shown to be well-defined in all the energy range and shows a cusp-like singularity at the origin. Further approximations on our semiclassical expansions allow us to demonstrate that the unbounded conductance fluctuations grow linearly with the incoming Fermi wave-vector k. In the conclusions (Sect. 6) we analyze the experimental relevance of our findings and the implications for other integrable geometries.

Transport through a square cavity has recently been considered by Wirtz *et al.* [11], where alternative forms of the transmission coefficient were proposed and the correspondence between quantum results and classical trajectories was established. The dynamics through rectangular cavities constitutes a paradigm for the interplay between scattering and integrability, and has been treated in other contexts. For instance, it has been presented by Zwanzig [27] as an example where the short memory approximation to the migration of a classical dynamical system between regions of configuration space is entirely wrong.

2 Semiclassical formulation

We consider a phase-coherent cavity connected to two reservoirs through leads that support N propagating modes. The conductance in the Landauer formalism is proportional to the transmission coefficient T

$$g = \frac{e^2}{h}\, T = \frac{e^2}{h} \sum_{a,b=1}^{N} |t_{ba}|^2. \tag{1}$$

The complex numbers t_{ba} are the transmission amplitudes from the mode a at the entrance lead to the mode b at the exit lead. They are related to the Green function (evaluated at the Fermi energy $E_{\rm F}$) connecting the point $(0, y)$ at the entrance with (L, y') at the exiting lead through [28]:

$$t_{ba} = -\mathrm{i}\hbar\sqrt{v_a v_b} \iint \mathrm{d}y\, \mathrm{d}y'\, \phi_b^*(y')\, \phi_a(y) \times G(L, y'; 0, y\,; E_{\rm F}), \tag{2}$$

where we have discarded an unimportant phase factor. $\phi_{a,b}$ represent the transverse wave functions in the leads of width W ($\phi_a(y) = \sqrt{2/W}\sin(a\pi y/W)$) and $v_{a,b}$ the longitudinal velocities associated with the modes a and b.

In the semiclassical approximation, the Green function is expressed as a sum over trajectories joining the points $(0, y)$ and (L, y') [3]:

$$G_{\rm scl}(L, y'; 0, y; E_{\rm F}) = \frac{2\pi}{(2\pi\mathrm{i}\hbar)^{3/2}} \sum_{s(y,y')} \sqrt{D_s} \times \exp\left[\frac{\mathrm{i}}{\hbar} S_s(y', y, E_{\rm F}) - \mathrm{i}\frac{\pi}{2}\mu_s\right]. \tag{3}$$

S_s is the classical action along the trajectory s. Since we are considering billiards without magnetic field $S_s = kL_s$,

with $k = mv/\hbar$ the Fermi wavevector and L_s the trajectory length. Denoting θ and θ' the incoming and outgoing angles, the preexponential factor is given by $D = (v\cos\theta'/m)^{-1}|(\partial\theta/\partial y')_y|$. We include in the phase μ_s the Maslov index counting the number of constant-energy conjugate points and the phase acquired at the bounces with the hard walls.

The semiclassical expression of the transmission amplitude is obtained by using the above approximation of the Green function in equation (2) and performing the y and y' integrals to leading order in $\hbar$. A stationary-phase integration over y selects the trajectories entering the cavity with the angle $\theta_{\bar{a}}$ ($\bar{a} = \pm a$ and $\sin\theta_{\bar{a}} = \bar{a}\pi/kW$) and leaving at the point y', leading to

$$t_{ba} = \mathrm{i}\sqrt{\frac{v_b}{2W}}\int \mathrm{d}y'\ \phi_b(y') \sum_{\bar{a}=\pm a}\sum_{s(\theta_{\bar{a}},y')} \mathrm{sgn}\,\bar{a}\sqrt{B_s} \times \exp\left[\frac{\mathrm{i}}{\hbar}\tilde{S}_s(y',\theta_{\bar{a}},E_\mathrm{F}) - \mathrm{i}\frac{\pi}{2}\tilde{\mu}_s\right]. \quad (4)$$

The reduced action is

$$\tilde{S}(y',\theta_{\bar{a}},E_\mathrm{F}) = S(y',y_0,E_\mathrm{F}) + \hbar\pi\bar{a}y_0/W\ , \quad (5)$$

where $y_0(\theta_{\bar{a}},y')$ is the initial point selected from the stationary-phase integration. The prefactor is now given by $B = (v\cos\theta')^{-1}|(\partial y/\partial y')_\theta|$, and the Maslov index is increased by one if $(\partial\theta/\partial y)_{y'}$ is positive.

When nearby trajectories are non-degenerate in action, as is typically the case in chaotic cavities, the integral over y' can also be done by stationary-phase and the semiclassical t_{ba} is expressed as a sum over trajectories with quantized initial and final angles [6,7]. On the other hand, when trajectories come in families with the same action (or length) the phase in equation (4) is linear in y', preventing another stationary-phase integration. This is the case of the trajectories directly crossing a ballistic cavity from the entrance to the exiting lead, where the y'-integral can be exactly done [7,9]. The trajectories going through a square cavity also come in families, or bundles [11], and the integration over the y'-coordinate is very similar to the case of direct trajectories since the dynamics in an extended space is that of free particles (Fig. 1).

Symmetry arguments for a rectangular cavity dictate that $t_{ba}=0$ if $a+b$ is odd. For even $a+b$ we perform the y'-integration for each family n defined by the coordinates (p_n,q_n) of the exiting lead in the extended space obtaining

$$t_{ba} = -\frac{\mathrm{i}}{\mathrm{W}}\sqrt{\frac{\cos\theta_b}{\cos\theta_a}}\sum_n \{I_n(a+b) - I_n(a-b)\} \times \exp\left[\mathrm{i}\left(kL_n + \frac{\pi a}{W}(q_n - L_n\sin\theta_a + W\varepsilon(q_n)) - \frac{\pi}{2}\tilde{\mu}_n\right)\right] \quad (6)$$

where

$$I_n(x) = \frac{W}{\pi x}\left(\exp\left[\frac{\mathrm{i}\pi x}{W}y_\mathrm{f}^{\prime(n)}\right] - \exp\left[\frac{\mathrm{i}\pi x}{W}y_\mathrm{i}^{\prime(n)}\right]\right). \quad (7)$$

$y_\mathrm{i}^{\prime(n)}$ and $y_\mathrm{f}^{\prime(n)}$ are the extreme points of the exiting interval, $\varepsilon(q_n)=0$ for even q_n and $\varepsilon(q_n)=1$ for odd q_n. The parity of q_n appears in the phase due to mirror symmetries involved in going to the extended space. The trajectories of the nth family have a length $L_n = p_n/\cos\theta_a$ (all lengths are expressed in units of the side of the square). In the extended space we have free motion, therefore the phase $\tilde{\mu}_n$ is simply given by the p_n-1 bounces with the vertical walls and the q_n bounces with the horizontal ones; that is, $\tilde{\mu}_n = 2(p_n+q_n-1)$. The trajectories that contribute to the transmission amplitude are those going from the left to the right lead, therefore only the values n with odd p_n should be considered. Conversely, the even values of p_n yield the reflection amplitude. For transmission amplitude we can simplify the phase of equation (6) and write

$$t_{ba} = -\frac{\mathrm{i}}{\mathrm{W}}\sqrt{\frac{\cos\theta_b}{\cos\theta_a}}\sum_n \varepsilon_n \exp[\mathrm{i}k\tilde{L}_n]\,\{I_n(a+b) - I_n(a-b)\}\,. \quad (8)$$

We have defined the phase

$$\varepsilon_n = \exp[\mathrm{i}\pi(a+1)\varepsilon(q_n)]\ , \quad (9)$$

and the reduced length

$$\tilde{L}_n = p_n\cos\theta_a + q_n\sin\theta_a\ . \quad (10)$$

Similarly to the case of direct trajectories [7], $\bar{a}+\bar{b}=0$ has to be treated separately for the y'-integration. However, the corresponding result is included in equation (8) by taking the limit $x\to 0$. Obviously, $\bar{a}+\bar{b}=0$ corresponds to the maximum transmission since this is the case where the classical trajectory arrives to the exiting lead with the quantized angle of mode b. As emphasized in reference [11], the diffractive terms obtained for $\bar{a}+\bar{b}\neq 0$ become more important for families with a weight $\delta_n = y_\mathrm{f}^{\prime(n)} - y_\mathrm{i}^{\prime(n)} \ll W$.

3 Continued fraction representation

In order to calculate the semiclassical transmission amplitude of equation (8) we need to determine all families n, with their exiting lead (p_n,q_n) and extreme points $y_{\mathrm{f,i}}^{\prime(n)}$. This evaluation naturally leads to a diophantic problem [30]. As we show below, the coefficients (p_n,q_n) are part of the intermediate fractions (or Farey series) appearing in the continued fraction representation of $1/\tan\theta_{\bar{a}}$.

For a given angle θ and an initial point y_0, the trajectory in extended space is the straight line $D(y_0)$ defined by $y = y_0 + x\tan\theta$. Let us start with the trajectory entering the cavity at the lowest point ($y_0=0$), whose exiting lead is defined by the segment $[(p_0,q_0);(p_0,q_0+W)]$ which intersects $D(0)$ (see Fig. 1). As we increase y_0, we will remain within a family of degenerate trajectories (that we note by $n=0$) until the exiting point $y_0+p_0\tan\theta$ hits the uppermost point of the segment. The pair (p_0,q_0) must

verify the conditions:

a. $0 < p_0 \tan\theta - q_0 < W$,
b. $\forall (p,q)$ such that

$$0 < p\tan\theta - q < p_0\tan\theta - q_0 \Rightarrow p > p_0.$$

According to a, the first y-interval is $[0, \delta_0]$ (or equivalently, the first y'-interval is $[W-\delta_0, W]$), while condition b means that (p_0, q_0) is the first lattice point verifying a. The uppermost family will be associated with an interval $[(p_0^*, q_0^*); (p_0^*, q_0^* + W)]$, where the pair (p_0^*, q_0^*) verifies similar conditions as (p_0, q_0):

c. $0 < W + p_0^*\tan\theta - q_0^* < W$,
d. $\forall (p,q)$ such that

$$W + p_0^*\tan\theta - q_0^* < W + p\tan\theta - q < W \Rightarrow p > p_0^*.$$

According to c, the first y-interval of the uppermost family is $[W-\delta_0^*, W]$ (the first y'-interval is $[0, \delta_0^*]$), while d implies that (p_0^*, q_0^*) is the first lattice point verifying c.

Now that we have determined the lowest and the uppermost families for the $[0, W]$ y-interval, the following sequences of families can be obtained by reducing ourselves to the y-interval $[\delta_0, W-\delta_0^*]$, and with the changes of (p_0, q_0), (p_0^*, q_0^*) by (p_1, q_1), (p_1^*, q_1^*) the conditions $a-d$ define the next two families. Continuing this procedure until the two sequences of families begin to overlap each other, we obtain all the terms to be included in the sum of equation (8). For the sequence of lower families we have

$$y'_{\rm i}(p_l, q_l) = W + (p_l - p_{l-1})\tan\theta - (q_l - q_{l-1}), \quad (11a)$$

$$y'_{\rm f}(p_l, q_l) = W, \quad (11b)$$

$$\delta_l = y'_{\rm f} - y'_{\rm i} = q_l - q_{l-1} - (p_l - p_{l-1})\tan\theta, \quad (11c)$$

while for the upper-families we have

$$y'_{\rm i}(p_u^*, q_u^*) = 0, \quad (12a)$$

$$y'_{\rm f}(p_l^*, q_l^*) = (p_u^* - p_{u-1}^*)\tan\theta - (q_u^* - q_{u-1}^*), \quad (12b)$$

$$\delta_u^* = (p_u^* - p_{u-1}^*)\tan\theta - (q_u^* - q_{u-1}^*). \quad (12c)$$

The very last family is simultaneously shadowed by lower and upper families, therefore has $y'_{\rm i}$ given by (11a) and $y'_{\rm f}$ by (12b).

We can now establish the relationship with the continued fraction representation of $\Theta = 1/\tan\theta$, that is defined by the sequences (α_m) and (a_m) as follows [30]:

$$\begin{array}{cc} \alpha_0 = \Theta & a_0 = [\alpha_0] \\ \alpha_{m+1} = \dfrac{1}{\alpha_m - a_m} & a_{m+1} = [\alpha_{m+1}]. \end{array} \quad (13)$$

$[\alpha]$ denotes the integer part of α. The best rational approximations to Θ are the fractions P_m/Q_m, called convergents, and obtained from the recurrence relations

$$\begin{cases} P_m = P_{m-2} + a_m P_{m-1} \\ Q_m = Q_{m-2} + a_m Q_{m-1}, \end{cases} \quad (14)$$

with the initial choice of $(P_{-1}, Q_{-1}) = (1, 0)$ and $(P_0, Q_0) = ([\Theta], 1)$. Since (P_m) and (Q_m) are sequences of integers, we can represent the convergents as lattice points (P_m, Q_m) that approach the straight line $D(0)$ as m increases from above (even m) and below (odd m). Moreover, the convergents verify

e. $\forall (p,q)$ such that

$$|p\tan\theta - q| < |P_m\tan\theta - Q_m| \Rightarrow p > P_m.$$

The intermediate lattice points on the segment $[(P_{m-2}, Q_{m-2}), (P_m, Q_m)])$ define the m th Farey sequence (or intermediate fractions) by

$$\begin{cases} p_m^k = P_{m-2} + kP_{m-1} \\ q_m^k = Q_{m-2} + kQ_{m-1} \end{cases} \quad 0 \le k \le a_m. \quad (15)$$

The sequence of equally spaced lattice points (p_m^k, q_m^k) starts at the convergent (P_{m-2}, Q_{m-2}) (for $k=0$) and finishes at (P_m, Q_m) (for $k=a_m$). The translation vector is given by the coordinates of the convergent (P_{m-1}, Q_{m-1}) and the intermediate fractions verify the properties

f. $\forall m, k, (p,q)$ such that

$$0 < p\tan\theta - q < p_{2m+1}^k\tan\theta - q_{2m+1}^k \Rightarrow p > p_{2m+1}^k,$$

g. $\forall m, k, (p,q)$ such that

$$q_{2m}^k - p_{2m}^k\tan\theta > q - p\tan\theta > 0 \Rightarrow p > p_{2m}^k.$$

These are the conditions b and d, respectively, determining the lattice points associated with the exiting leads. Therefore, the two types of families contributing to t_{ba} are given by the Farey sequences of even and odd order convergents, with the the additional requirements that p_n is odd and that the exiting points are closer than W to the straight line $D(0)$.

The continued fraction representation of a generic (irrational) real number results in an infinite sequence of convergents. However, the fact that we have defined a finite distance W to approach $D(0)$ implies that once the lower and upper families begin to overlap the sum in equation (8) can be cut. Therefore, for each angle θ_a the sum is actually finite. In addition, we show in the sequel that at most three sequences of intermediate fractions contribute to it. Let us consider the first convergent (P_m, Q_m) contributing to the sum (the previous convergents being farther away than W to $D(0)$), and assume for definiteness m to be odd. Clearly, before this convergent we can only have one contributing Farey sequence:

$$(p_m^k, q_m^k) \quad \text{with} \quad k \in (1, a_m). \quad (16)$$

The $k = 0$ case is excluded because otherwise (P_m, Q_m) would not be the first convergent of the sum. The following sequence,

$$(p^k_{m+1}, q^k_{m+1}) \quad \text{with} \quad k \in (1, a_{m+1}), \tag{17}$$

is relevant since it finishes at the next convergent $(P_{m+1}, Q_{m+1}) = (p^{m+1}_{m+1}, q^{m+1}_{m+1})$, which must contribute to the sum. It is closer to $D(0)$ than (P_m, Q_m)) and it is not completely shadowed by (P_m, Q_m) (they are at opposite sides of $D(0)$). Consequently, there are two possibilities: (i) (P_{m+1}, Q_{m+1}) is partially shadowed by (P_m, Q_m) and therefore the sum stops there since the points (p^k_{m+2}, q^k_{m+2}) with $k > 0$ will be completely shadowed; (ii) (P_{m+1}, Q_{m+1}) is not shadowed by (P_m, Q_m), therefore (p^1_{m+2}, q^1_{m+2}) is simultaneously shadowed by (P_m, Q_m) and (P_{m+1}, Q_{m+1}) since $W + q^1_{m+2} - p^1_{m+2} \tan\theta > Q_{m+1} - P_{m+1} \tan\theta > 0$ is equivalent to $W + Q_m - P_m \tan\theta > 0$, which is precisely the condition for (P_m, Q_m) being an exiting point. The points (p^k_{m+2}, q^k_{m+2}) with $k > 1$ are completely shadowed, and therefore the series stops there. In conclusion, in the case (i) the contributing Farey sequences are those of equations (16, 17), while in case (ii) we have to add one intermediate fraction of the next family, namely (p^1_{m+2}, q^1_{m+2}).

The above considerations simplify the semiclassical transmission amplitude of equation (8) to a finite sum, having at most three sequences of intermediate fractions. In case (i) the form of the y'-intervals (Eqs. (11, 12)) is $[W - \delta_l, W]$ or $[0, \delta^*_u]$, therefore equation (8) can be written as

$$t_{ba} = \frac{1}{W}\sqrt{\frac{\cos\theta_b}{\cos\theta_a}} \sum_{n=l,u} \varepsilon_n \varepsilon'_n \exp\left[\mathrm{i}k\tilde{L}_n\right] \times \left\{\Delta_n(a+b) - \Delta_n(a-b)\right\} \delta_n, \tag{18}$$

with the family-dependent function Δ_n defined by

$$\Delta_n(x) = \frac{2W}{\pi x \delta_n} \exp\left[\mathrm{i}\frac{\pi x \delta_n}{2W}\right] \sin\left[\frac{\pi x \delta_n}{2W}\right], \tag{19}$$

$\varepsilon'_n = 1$ if $n = u$ (upper family) and $\varepsilon'_n = -1$ if $n = l$ (lower family). As previously stated, only odd p_n should be considered in the expansion for the transmission amplitude. In case (ii) the last family does not have a y'-interval with the simple form of the previous ones. Therefore, equation (18) depending only on the weights δ_n can be used for all terms (families of trajectories), except for the last one, were the form (8) together with the limits (11a) and (12b) should be employed. However, for the last family the weight $\delta(p^1_m, q^1_m)$ is very small and to first order in $(a \pm b)\delta(p^1_m, q^1_m)/W$, we can still use equation (18). We stress that the subindex n runs over contributing families, while m labels the convergents (contributing or not) and the superindex k orders the intermediate fractions of the Farey sequences.

The forms (8) and (18) of the transmission amplitude provide a very powerful method to numerically compute the conductance through a rectangular cavity. For each $a = 1, \ \ldots, \ N$, we only need to calculate a finite number of convergents and intermediate fractions of the continued fraction representation of $1/\tan\theta_a$ and recursively obtain the weighting intervals δ_n. The advantage over quantum methods based on discretization (recursive Green function, wave function matching, etc.) is that it can be used for large wavevectors k. The method actually gets more exact with increasing k since it involves a semiclassical approximation. Obviously, equation (18) does not incorporate diffractive effects like reflection off the lead mouths [8,10,29]. However, as shown in reference [10], the semiclassical approach can be adapted in order to describe these simple diffractive effects.

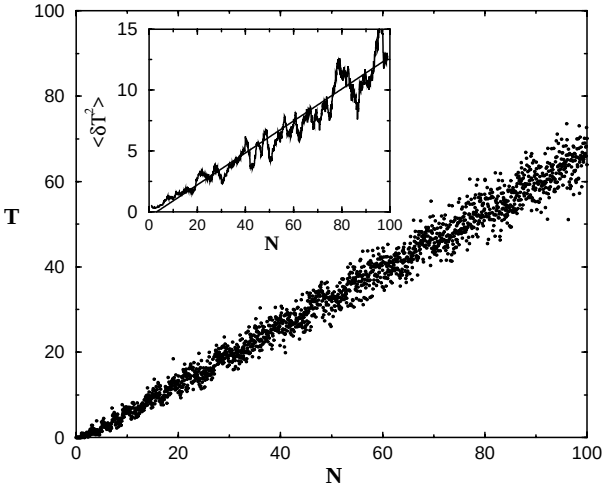

Fig. 2. Conductance through a square cavity in units of e^2/h as a function of the number of modes $N = kW/\pi$ for an opening of $W = 0.2$ in units of the size of the square. Inset: local average of the conductance fluctuations $\langle \delta T^2 \rangle$ *versus* N. The straight line is the local variance of the fluctuations computed from equation (31).

In Figure 2 we present the conductance of a square cavity calculated from equation (18) for an opening $W = 0.2$ in a large k-interval (the k-mesh shown is relatively sparse for viewing purposes). We remark two salient features: the linear increase of the mean conductance with $N = kW/\pi$ and the fluctuations around the mean, which become larger as k increases. The linear increase of $\langle g \rangle$ with a slope given by the classical transmission coefficient constitutes a checking of the procedure, the increase of the fluctuations obtained within our semiclassical approach is consistent with previous quantum computations [7]. In the following section we show that further approximations on the semiclassical transmission amplitudes t_{ba} allow us to obtain both these features analytically.

As it has been shown in previous studies comparing semiclassical and quantum results [8,10,11], the former reproduce the gross structure of the fluctuations in the intermediate k-regime (not too small k in order for semiclassics to apply and not too large k to prevent the quantum calculations becoming unreliable). The quantum-semiclassical correspondence is particularly clear at the level of the Fourier components of the transmission coefficients. Specifically, for square cavities Wirtz *et al.* [11]

have identified the peaks of the Fourier transforms with the families (or bundles) of classical trajectories contributing in a semiclassical expansion. Unitarity, the mathematical translation of charge conservation, is a critical test for semiclassical approximations. In our case, the difference $T+R-N$ grows with N, but it remains smaller than the fluctuations of T.

4 Mean conductance

The semiclassical expression (18) for the transmission amplitude is very useful since, as we have shown in the previous chapters, the numerical evaluation of a few continued fractions allows the calculation of the conductance. In the sequel we further simplify this semiclassical approach in order to render it analytically tractable. The function $\Delta_n(x)$ defined in equation (19) is peaked for $x=0$ (when the quantized angles of the incoming and outgoing modes coincide with the angle of the trajectory) and decays on the scale of W/δ_n, therefore it can be approximated by the rectangular function

$$\Pi_n(x) = \begin{cases} \exp\left[\mathrm{i}\dfrac{\pi x \delta_n}{2W}\right] & \text{if} \quad |x| < \frac{W}{2\delta_n}, \\ 0 & \text{otherwise.} \end{cases}$$

Thus, the semiclassical t_{ba} simplifies to:

$$t_{ba} = \frac{1}{W}\sqrt{\frac{\cos\theta_b}{\cos\theta_a}} \sum_n \Pi_n(a-b)\varepsilon_n\varepsilon'_n\delta_n \exp[\mathrm{i}k\tilde{L}_n]. \quad (20)$$

The total transmission coefficient is obtained by summing the magnitude squared of the transmission amplitudes over the propagating modes. Therefore, within our semiclassical approximation, it will be expressed as a sum over pairs of families of trajectories (with odd p_n and $p_{n'}$).

$$T = \frac{1}{W^2}\sum_{a,b=1}^{N} \frac{\cos\theta_b}{\cos\theta_a} \sum_{n,n'} \varepsilon_n\overline{\varepsilon}_{n'}\varepsilon'_n\varepsilon'_{n'}\delta_n\delta_{n'} \times \exp\left[\mathrm{i}k(\tilde{L}_n - \tilde{L}_{n'})\right]\Pi_n(a-b)\overline{\Pi}_{n'}(a-b). \quad (21)$$

From this highly oscillating function of k, we want to extract its secular behavior, linear in k. Averaging $T(k)/k$ over all k [7] (or $T(k)$ over several oscillations) amounts to make the diagonal approximation between the families of trajectories ($n = n'$). In the well-studied case of isolated trajectories, the diagonal approximation yields the classical probability of transmission by pairing individual trajectories. In the present case, the concept of families of trajectories replaces the role of individual trajectories. Inserting the definition of the function Π, we find

$$\langle T\rangle = \frac{1}{W^2}\sum_{a=1}^{N}\sum_n \delta_n^2 \left(\sum_{b=b_{\min}}^{b_{\max}} \frac{\cos\theta_b}{\cos\theta_a}\right), \quad (22)$$

$b_{\min} = \max\{a - W/2\delta_n, 1\}$ and $b_{\max} = \min\{a + W/2\delta_n, N\}$. We now split the sum over families according to

$$\langle T\rangle = \frac{1}{W^2}\sum_{a=1}^{N}\frac{1}{\cos\theta_a}\left[\sum_{0<\delta_n<\delta_\alpha}\delta_n^2\sum_{b=1}^{N}\cos\theta_b + \sum_{\delta_\alpha<\delta_n<\delta_\beta}\delta_n^2\sum_{b=b_{\min}}^{b_{\max}}\cos\theta_b + \sum_{\delta_n>\delta_\beta}\delta_n^2\sum_{b=a-W/2\delta_n}^{a+W/2\delta_n}\cos\theta_b\right] \quad (23)$$

with δ_α and δ_β respectively the min and max of $\{W/2a, W/2(N-a)\}$. In the classical limit of $N = kW/\pi \gg 1$ the last term dominates and the sum over b can be approximated by an integral leading to

$$\langle T\rangle = \sum_{a=1}^{N}\sum_n \frac{\delta_n}{W}\,. \quad (24)$$

For each mode a we have simply obtained the total weight of trajectories contributing to transmission. In the classical limit the sum over a is converted into an integral over the initial angle θ and we write

$$\langle T\rangle = N\tau \quad (25)$$

with

$$\tau = \int_0^{\pi/2} \mathrm{d}\theta\cos\theta \sum_n \frac{\delta_n}{W}\,. \quad (26)$$

Therefore, the total transmission coefficient is proportional to the number of modes, and the constant τ is a purely geometric factor. Breaking the contribution of families into that of individual trajectories we are left with the usual classical transmission probability [7]

$$\tau = \frac{1}{2}\int_{-\pi/2}^{\pi/2}\mathrm{d}\theta\cos\theta\int_0^W \frac{\mathrm{d}y}{W}\; f(y,\theta), \quad (27)$$

where $f(y,\theta) = 1$ if the trajectory with initial conditions (y,θ) is transmitted and $f(y,\theta) = 0$ otherwise.

The mean slope in the numerical results of Figure 2 (with $W = 0.2$) is 0.67, in excellent agreement (better than 0.5%) with the classical transmission probability τ. Also, the local mean $\langle T(k)\rangle$ of equation (24) presents the same slope τ and the mode quantization gives rise to fluctuations around this mean (which remain much smaller than those of $T(k)$). The classical coefficient τ can be obtained, as in equation (27), by sampling the space of classical trajectories with random choices of initial conditions θ and y [7], or more efficiently, by sampling the angles θ and incorporating the weights δ_n emerging from the intermediate fractions of $1/\tan\theta$, as suggested by equation (26). We then see that the continued fraction approach is not only useful for evaluating semiclassical effects, but also for classical properties like the transmission coefficient or the

length distribution. Random sampling of classical trajectories is an appropriate procedure for chaotic structures, where the ergodicity of phase space results in an exponential distribution of lengths. On the other hand, integrable cavities exhibit power-law distributions, which are more difficult to obtain by trajectory sampling. In this case, the continued fraction approach is very efficient since, for a given angle, only a finite number of terms are relevant, and the contributing families are incorporated at once according to their weight.

The straight line that best approximates the transmission coefficient $T(k)$ is $\tau N + \kappa$. The constant κ is related with the elastic backscattering and also depends on the underlying classical dynamics. In particular, the dependence of κ on the magnetic field results in the weak localization effect [7,22]. However, we will not address the effect of a magnetic field in this work, nor the calculation of κ.

5 Conductance fluctuations

As visible from Figure 2, the oscillations around the mean transmission coefficient $\tau N + \kappa$ grow with larger N, consistently with the numerical quantum mechanical calculations of reference [7]. We will now evaluate the local fluctuations, that is $\langle \delta T^2 \rangle = \langle (T - (\tau N + \kappa))^2 \rangle$. We begin with the simplified expression (21) of T, and write

$$\begin{aligned} T^2 = \frac{1}{W^4} \sum_{a,b,a',b'=1}^{N} & \frac{\cos\theta_b}{\cos\theta_a} \frac{\cos\theta_{b'}}{\cos\theta_{a'}} \\ & \times \sum_{n,n',n'',n'''} \varepsilon_n \overline{\varepsilon}_{n'} \varepsilon_{n''} \overline{\varepsilon}_{n'''} \varepsilon'_n \overline{\varepsilon}'_{n'} \varepsilon'_{n''} \overline{\varepsilon}'_{n'''} \delta_n \delta_{n'} \delta_{n''} \delta_{n'''} \\ & \times \exp\left[ik(\tilde{L}_n - \tilde{L}_{n'} + \tilde{L}_{n''} - \tilde{L}_{n'''}) \right] \\ & \times \Pi_n(a-b) \overline{\Pi}_{n'}(a-b) \Pi_{n''}(a'-b') \overline{\Pi}_{n'''}(a'-b'). \end{aligned} \tag{28}$$

If we take the average over several fluctuations, we only consider the terms having a null phase, *i.e.*

$$\tilde{L}_n - \tilde{L}_{n'} + \tilde{L}_{n''} - \tilde{L}_{n'''} = 0. \tag{29}$$

This condition is satisfied with the pairing $\tilde{L}_n = \tilde{L}_{n'}$ and $\tilde{L}_{n''} = \tilde{L}_{n'''}$, but the resulting term cancels against the square of the average transmission coefficient. A non trivial pairing is obtained when $\tilde{L}_n = \tilde{L}_{n'''}$ and $\tilde{L}_{n'} = \tilde{L}_{n''}$ with $\tilde{L}_n \neq \tilde{L}_{n'}$, which implies $a = a'$. The contribution of this pairing to the local fluctuations is

$$\begin{aligned} \langle \delta T^2 \rangle_I &= \frac{1}{W^4} \sum_{a=1}^{N} \sum_{b,b'=1}^{N} \frac{\cos\theta_b \cos\theta_{b'}}{\cos^2\theta_a} \\ &\quad \times \sum_{n,n'} \Pi_n(a-b) \overline{\Pi}_{n'}(a-b) \Pi_{n'}(a-b') \overline{\Pi}_n(a-b') \delta_n^2 \delta_{n'}^2 \\ &= \frac{1}{W^4} \sum_{a=1}^{N} \sum_{n,n'} \left(\min\left\{ \frac{W}{\delta_n}, \frac{W}{\delta_{n'}} \right\} \right)^2 \delta_n^2 \delta_{n'}^2. \end{aligned} \tag{30}$$

In the semiclassical limit the sum over a can be converted into an integral dictating a linear behavior of $\langle \delta T^2 \rangle_I$ with respect to k

$$\langle \delta T^2 \rangle_I = \frac{N}{2} \int_{-\pi/2}^{\pi/2} \mathrm{d}\theta \cos\theta \sum_{n,n'} \left(\frac{\min\{\delta_n, \delta'_n\}}{W} \right)^2 . \tag{31}$$

The proportionality coefficient is only related to the geometry of the cavity, and can be computed using continued fractions.

The two pairings above described are those usually considered in dealing with chaotic cavities, except that in such cases we take individual trajectories instead families. In the integrable system we are studying there is another non trivial way of satisfying equation (29), that is, $\tilde{L}_n - \tilde{L}_{n'} = \tilde{L}_{n''} - \tilde{L}_{n'''}$, with $\tilde{L}_n \neq \tilde{L}_{n'}$ and $\tilde{L}_n \neq \tilde{L}_{n''}$. This typically happens when n, n', n'', and n''' belong to the same (mth) Farey sequence and they are respectively associated with the intermediate functions (p_m^{k+j}, q_m^{k+j}), (p_m^k, q_m^k), $(p_m^{k'}, q_m^{k'})$, and $(p_m^{k'+j}, q_m^{k'+j})$, with $k \neq k'$, $j \neq 0$ and $k, k', k+j, k'+j \in (0, a_m)$. Also, since we are dealing with transmission coefficients, we need p_m^k, $p_m^{k'}$, p_m^{k+j} and $p_m^{k'+j}$ to be odd, which implies that if j is odd, P_{m-1} must be even. Under such conditions, according to equations (10, 15) we have

$$\tilde{L}_n - \tilde{L}_{n'} = j \left(P_{m-1} \cos\theta_a + Q_{m-1} \sin\theta_a \right). \tag{32}$$

If neither n nor n' correspond to the first family of the sequence ($k, k' \neq 0$), equations (11c, 12c, 15) dictate that the four exiting intervals have the same length

$$\delta_m = \left| P_{m-1} \tan\theta - Q_{m-1} \right|. \tag{33}$$

This last contribution to the local fluctuations can be expressed as a sum over the convergents

$$\langle \delta T^2 \rangle_{II} = \sum_{a=1}^{N} \sum_{m} \sum_{k,k'=0}^{a_m} \sum_{j} \frac{\delta_m^2}{W^2}, \tag{34}$$

with the above specified restrictions for k, k' and j. As in the previous case, converting the sum over a into an integral yields a contribution $\langle \delta T^2 \rangle_{II}$ to the local fluctuations that is linear in k, with a purely geometrical coefficient given by the continued fraction representation of $1/\tan\theta$.

The linearity of $\langle \delta T^2 \rangle = \langle \delta T^2 \rangle_I + \langle \delta T^2 \rangle_{II}$ with k that we have demonstrated is in good agreement with our numerical results of Figure 2. In the inset we show the numerically obtained $\langle \delta T^2 \rangle$ and the straight line representing $\langle \delta T^2 \rangle_I$ from equation (31), with a proportionality coefficient of 0.13 calculated from the continued fractions. The agreement is very good and shows that $\langle \delta T^2 \rangle_{II}$ is negligible in comparison with $\langle \delta T^2 \rangle_I$. Such behavior is understandable since, for a given incoming mode a, the latter is given by a double sum over families of trajectories (n and n'), while the former is given as a [single] sum over the convergents (m) and sums within the associated Farey sequence, provided it verifies the above established conditions. The denominators Q_m of the convergents increase

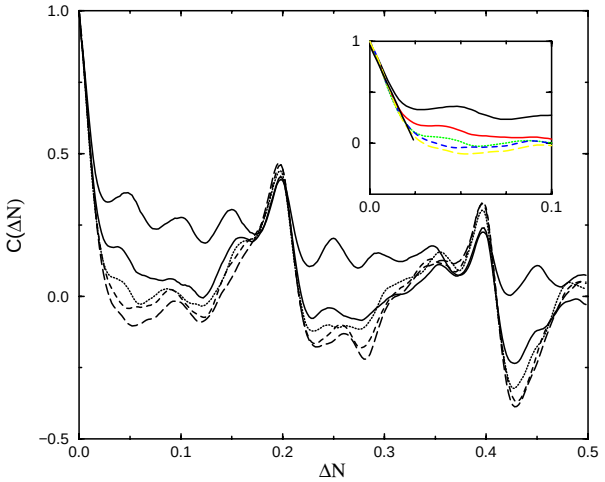

Fig. 3. Correlation function locally normalized according to equation (36) for five N intervals: 0–20 (thick solid), 20–40 (thin solid), 40–60 (dotted), 60–80 (dashed) and 80–100 (long-dashed). Inset: blow up of the small ΔN region showing a triangular behavior at the origin for all the intervals considered.

exponentially with m, $Q_m \geq 2^{(m-1)/2}$ [30], or more precisely as Greenman has recently proved [31]

$$\lim_{m\to\infty} Q_m^{1/m} = \exp\left[\frac{\pi^2}{12\log 2}\right], \tag{35}$$

bar a set of measure zero. Therefore, the a_m of equations (13, 14), giving the number of intermediate fractions of the mth sequence, remain of order 1 even in the large m-limit. Consequently, there are much more terms contributing to $\langle \delta T^2 \rangle_I$ than to $\langle \delta T^2 \rangle_{II}$.

In chaotic cavities the diagonal approximation is not enough to describe the magnitude of the conductance fluctuations, due to the exponential proliferation of trajectories that results in almost degenerate actions. This is clearly not the case in rectangular cavities, where we have shown the good agreement between $\langle \delta T^2 \rangle_I$ and the numerical results.

Conductance fluctuations are usually characterized by their amplitude $\langle \delta T^2 \rangle$ and their energy-correlation length. In chaotic cavities, random matrix theory and numerical simulations [19,20] yield an universal $\langle \delta T^2 \rangle$, independent of energy. The correlation length can be obtained from a semiclassical approach [6,18] and is proportional to the escape rate (the inverse characteristic time that scattering trajectories spend in the cavity). In our integrable cavity we have seen that $\langle \delta T^2 \rangle$ is not universal, but energy dependent. Also, there does not exist a characteristic time for exiting the cavity. Therefore it is not obvious that a correlation function depending only on the energy increment can be defined. That is why we consider the correlation function

$$C(\Delta k) = \frac{\langle \delta T(k+\Delta k)\delta T(k)\rangle}{\langle \delta T^2(k)\rangle}, \tag{36}$$

where k varies on an interval much larger than Δk, but small enough to neglect secular variations.

From equations (36, 18) we obtain numerically the correlation functions shown in Figure 3 for various N intervals from 0–20 (thick solid) to 80–100 (long-dashed). Except for the first interval, where the semiclassical approximation is most questionable, the form of $C(\Delta k)$ seems to be almost independent of the region of evaluation. Moreover, a singularity for small Δk appears in all the N-intervals in the form of a cusp around the origin (inset). The linear behavior of $C(\Delta k)$ is to be contrasted to the Lorentzian correlation function expected for a chaotic cavity. This difference between integrable and chaotic cavities is reminiscent of what happens with the weak localization effect: a semiclassical approach predicts a linear magneto resistance for integrable cavities and a Lorentzian lineshape for chaotic ones [22]. The linear behavior of the correlation function is consistent with the quantum calculations of reference [7] that yielded a decay of the power spectrum (Fourier transform of $C(\Delta k)$) as x^{-2} at large x.

The oscillatory structure of $C(\Delta N)$ on the scale of $\Delta N \simeq 0.2$ corresponds to a typical length of twice the size of the square. We can understand this behavior by noticing that, for a given angle θ, the smallest possible difference between the length of two trajectories is 2. The analytical calculation of $C(\Delta k)$ is considerably more involved than that of $\langle \delta T^2 \rangle$; we will have a sum as in equation (30), where each term should be multiplied by $\exp[i\Delta k(\tilde{L}_n - \tilde{L}_{n'})]$. Therefore it looks rather difficult to extract analytically the triangular behavior around the origin.

6 Conclusions

In this work we have developed a semiclassical method to calculate the transmission through a rectangular cavity, based on continued fractions. We have proved that the expansions, over families of trajectories, are finite and reproduce the basic features of quantum mechanical calculations. The conductance fluctuations, within our semiclassical approximation, are shown to be qualitatively different from the chaotic case: they increase linearly with the incoming Fermi wave-vector (with a proportionality coefficient that can be easily obtained with our scheme) and the correlation function presents a cusp-like singularity at the origin. The continued fraction approach is also useful to address classical properties like the transmission coefficient, the length distribution, or the area distribution (responsible for the the shape and magnetic field scale of the weak-localization effect).

We have seen that open systems exhibit larger fluctuations when the classical dynamics is integrable. The situation is analogous to the density of states of closed systems, which is characterized by stronger fluctuations in integrable than in chaotic geometries. The augmented fluctuations in *integrable closed and open* geometries can be traced to the same origin: *the bunching of trajectories into families* in the semiclassical expansions, the Berry-Tabor formula and equation (18) respectively.

In the example discussed in this work the classical dynamics in the leads has the same conserved quantities than

in the cavity, leading to bunching of trajectories in families of degenerate action. This is not the case in circular cavities, where a semiclassical expansion based on individual trajectories has been developed [9]. Therefore, the geometry of the leads plays a very important role [26] and renders the quantum signatures of integrability in open systems quite involved.

The existing experimental results [12,17] show the difference in the conductance fluctuations of integrable and chaotic cavities, but more work should be undertaken to test our results. The variation of Fermi energy (or number of modes N) has been achieved in chaotic and integrable ballistic microstructures [16,32]. However, the intervals ΔN of variation remain much smaller than those allowing to detect a linear increase of the variance. Therefore, microwave cavities [15] appear as more promising for the observation of such an effect.

We are indebted to H. Baranger, K. Richter and D. Ullmo for important remarks on the manuscript. We thank J. Bellisard and J. Keating for helpful hints on continued fractions.

References

1. *Chaos and Quantum Physics*, edited by M.-J. Giannoni, A. Voros, J. Zinn-Justin (North-Holland, Amsterdam, 1991).
2. O. Bohigas, M.J. Giannoni, C. Schmit, Phys. Rev. Lett. **52**, 1 (1984); O. Bohigas in reference [1], p. 87.
3. M.C. Gutzwiller, *Chaos in Classical and Quantum Mechanics* (Springer, Berlin, 1990); reference [1], p. 201.
4. M.V. Berry, M. Tabor, J. Phys. A **10**, 371 (1977).
5. W.H. Miller, Adv. Chem. Phys. **25**, 69 (1974).
6. R.A. Jalabert, H.U. Baranger, A.D. Stone, Phys. Rev. Lett. **65**, 2442 (1990).
7. H.U. Baranger, R.A. Jalabert, A.D. Stone, Chaos **3**, 665 (1993).
8. H. Ishio, J. Burgdörfer, Phys. Rev. B **51**, 2013 (1995).
9. W.A. Lin, R. Jensen, Phys. Rev. B **53**, 3638 (1996); W.A. Lin, Chaos, Solitons & Fractals **8**, 995 (1997).
10. C.D. Schwieters, J.A. Alford, J.B. Delos, Phys. Rev. B **54**, 10652 (1996).
11. L. Wirtz, J.-Z. Tang, J. Burgdörfer, Phys. Rev. B **56**, 7589 (1997).
12. C.M. Marcus *et al.*, Phys. Rev. Lett. **69**, 506 (1992); Chaos **3**, 643 (1993).
13. *Nanotechnology*, edited by B. Timp (AIP Press, 1995).
14. *Chaos and Quantum Transport in Mesoscopic Cosmos*, special issue, Chaos, Solitons & Fractals **8**, 971 (1997).
15. H.-J. Stöckmann, J. Stein, Phys. Rev. Lett. **64**, 2215 (1990); H.-D. Gräf *et al.*, Phys. Rev. Lett. **69**, 1296 (1992); M. Kollmann *et al.*, Phys. Rev. E **49**, R1 (1994).
16. M.W. Keller *et al.*, Surf. Sci. **305**, 501 (1994); Phys. Rev. B **53**, R1693 (1996).
17. Y. Lee, G. Faini, D. Mailly, Phys. Rev. B, **56**, 9805 (1997); reference [14], p. 1325.
18. R. Blümel, U. Smilansky, Phys. Rev. Lett. **64**, 241 (1990).
19. H.U. Baranger, P.A. Mello, Phys. Rev. Lett. **73**, 142 (1994); H.U. Baranger in reference [13].
20. R.A. Jalabert, J.-L. Pichard, C.W.J. Beenakker, Europhys. Lett. **27**, 255 (1994); C.W.J. Beenakker, Rev. Mod. Phys. **69**, 731 (1997).
21. A.G. Huibers *et al.*, Phys. Rev. Lett. **81**, 1917 (1998); C.M. Marcus *et al.*, reference [14], p. 1261.
22. H.U. Baranger, R.A. Jalabert, A.D. Stone, Phys. Rev. Lett. **70**, 3876 (1993).
23. A.M. Chang, H.U. Baranger, L.N. Pfeiffer, K.W. West, Phys. Rev. Lett. **73**, 2111 (1994); A.M. Chang, reference [14], p. 1281.
24. M.J. Berry, J.H. Baskey, R.M. Westervelt, A.C. Gossard, Phys. Rev. B **50**, 8857 (1994).
25. G. Lütjering *et al.*, Surf. Sci. **361/362**, 709 (1996).
26. J.P. Bird *et al.*, Phys. Rev. B **52**, R14336 (1995); reference [14], p. 1299.
27. R. Zwanzig, J. Stat. Phys. **30**, 255 (1983).
28. D.S. Fisher, P.A. Lee, Phys. Rev. B **23**, 6851 (1981).
29. M. Schreier, K. Richter, G.-L. Ingold, R.A. Jalabert, Eur. Phys. J. B **3**, 387 (1998).
30. A.Ya. Khinchin, *Continued Fractions* (University of Chicago Press, Chicago, 1964).
31. C. Greenman, J. Phys. A **30**, 915 (1997).
32. I.V. Zozoulenko, R. Schuster, K.-F. Berggren, K. Ensslin, Phys. Rev. B **55**, R10209 (1997).